US009219632B2

(12) **United States Patent**
Eliaz et al.

(10) **Patent No.: US 9,219,632 B2**
(45) **Date of Patent: Dec. 22, 2015**

(54) **HIGHLY-SPECTRALLY-EFFICIENT TRANSMISSION USING ORTHOGONAL FREQUENCY DIVISION MULTIPLEXING**

(71) Applicant: **MagnaCom Ltd.**, Moshav Ben Shemen (IL)

(72) Inventors: **Amir Eliaz**, Moshav Ben Shemen (IL); **Ilan Reuven**, Ganey Tikva (IL)

(73) Assignee: **MagnaCom Ltd.** (IL)

(*) Notice: Subject to any disclaimer, the term of this patent is extended or adjusted under 35 U.S.C. 154(b) by 0 days.

(21) Appl. No.: **14/329,100**

(22) Filed: **Jul. 11, 2014**

(65) **Prior Publication Data**

US 2015/0010108 A1 Jan. 8, 2015

Related U.S. Application Data

(63) Continuation of application No. 13/921,665, filed on Jun. 19, 2013, now Pat. No. 8,781,008, which is a continuation-in-part of application No. 13/755,008, filed on Jan. 31, 2013, now Pat. No. 8,571,131.

(Continued)

(51) **Int. Cl.**
H04K 1/02 (2006.01)
H04L 27/26 (2006.01)
(Continued)

(52) **U.S. Cl.**
CPC ***H04L 27/2697*** (2013.01); ***H04L 1/0042*** (2013.01); ***H04L 5/0044*** (2013.01); ***H04L 5/0098*** (2013.01); ***H04L 27/265*** (2013.01); ***H04L 27/2626*** (2013.01); ***H04L 27/2628*** (2013.01); ***H04L 27/2646*** (2013.01); ***H04L 27/2647*** (2013.01); ***H04L 27/2657*** (2013.01);

(Continued)

(58) **Field of Classification Search**
CPC H04L 1/0036
USPC 375/296
See application file for complete search history.

(56) **References Cited**

U.S. PATENT DOCUMENTS

4,109,101 A 8/1978 Mitani
4,135,057 A 1/1979 Bayless, Sr. et al.
(Continued)

FOREIGN PATENT DOCUMENTS

WO 2013/030815 A1 3/2013

OTHER PUBLICATIONS

Equalization: The Correction and Analysis of Degraded Signals, White Paper, Agilent Technologies, Ransom Stephens V1.0, Aug. 15, 2005 (12 pages).

(Continued)

Primary Examiner — Lihong Yu
(74) *Attorney, Agent, or Firm* — McAndrews, Held & Malloy, Ltd.

(57) **ABSTRACT**

A system may comprise a symbol mapper circuit that outputs C' quadrature amplitude modulation (QAM) symbols per orthogonal frequency division multiplexing (OFDM) symbol. The system may also comprise circuitry operable to process said C' QAM symbols using a circulant matrix to generate a particular OFDM symbol consisting of C+Δ subcarriers, where C' is a first integer, C is a second integer less than C', and Δ is an integer equal to the number of non-data-carrying subcarriers in the particular OFDM symbol. The circulant matrix may be a P×P matrix, where P is an integer less than C'. The system may comprise a nonlinear circuit that introduces nonlinear distortion to said particular OFDM symbol.

16 Claims, 8 Drawing Sheets

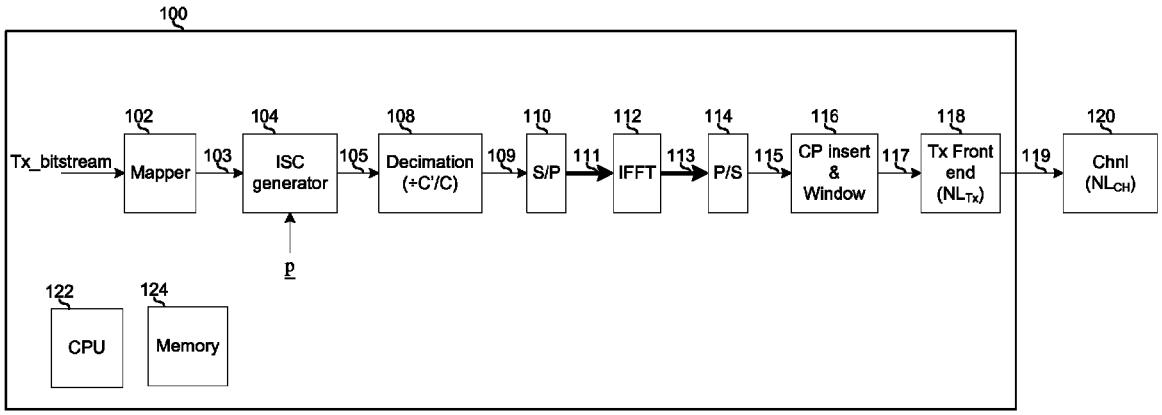

Related U.S. Application Data

(60) Provisional application No. 61/662,085, filed on Jun. 20, 2012, provisional application No. 61/726,099, filed on Nov. 14, 2012, provisional application No. 61/729,774, filed on Nov. 26, 2012, provisional application No. 61/747,132, filed on Dec. 28, 2012, provisional application No. 61/768,532, filed on Feb. 24, 2013, provisional application No. 61/807,813, filed on Apr. 3, 2013.

(51) **Int. Cl.**

H04L 1/00	(2006.01)
H04L 5/00	(2006.01)
H04L 25/03	(2006.01)
H04L 27/00	(2006.01)
H04L 1/06	(2006.01)

(52) **U.S. Cl.**

CPC *H04L 1/0071* (2013.01); *H04L 1/06* (2013.01); *H04L 5/006* (2013.01); *H04L 25/03159* (2013.01); *H04L 2027/003* (2013.01); *H04L 2027/0053* (2013.01); *H04L 2027/0067* (2013.01)

(56) **References Cited**

U.S. PATENT DOCUMENTS

4,797,925	A	1/1989	Lin	
5,111,484	A	5/1992	Karabinis	
5,131,011	A	7/1992	Bergmans et al.	
5,202,903	A	4/1993	Okanoue	
5,249,200	A	9/1993	Chen et al.	
5,283,813	A	2/1994	Shalvi et al.	
5,291,516	A	3/1994	Dixon et al.	
5,394,439	A	2/1995	Hemmati	
5,432,822	A	7/1995	Kaewell, Jr.	
5,459,762	A	10/1995	Wang et al.	
5,590,121	A	12/1996	Geigel et al.	
5,602,507	A	2/1997	Suzuki	
5,757,855	A	5/1998	Strolle et al.	
5,784,415	A	7/1998	Chevillat et al.	
5,818,653	A	10/1998	Park et al.	
5,886,748	A	3/1999	Lee	
5,889,823	A	3/1999	Agazzi et al.	
5,915,213	A	6/1999	Iwatsuki et al.	
5,930,309	A	7/1999	Knutson et al.	
6,009,120	A	12/1999	Nobakht	
6,167,079	A	12/2000	Kinnunen et al.	
6,233,709	B1	5/2001	Zhang et al.	
6,272,173	B1	8/2001	Hatamian	
6,335,954	B1	1/2002	Bottomley et al.	
6,356,586	B1	3/2002	Krishnamoorthy et al.	
6,516,437	B1	2/2003	Van Stralen et al.	
6,532,256	B2	3/2003	Miller	
6,535,549	B1	3/2003	Scott et al.	
6,690,754	B1	2/2004	Haratsch et al.	
6,697,441	B1	2/2004	Bottomley et al.	
6,785,342	B1	8/2004	Isaksen et al.	
6,871,208	B1	3/2005	Guo et al.	
6,968,021	B1	11/2005	White et al.	
6,985,709	B2	1/2006	Perets	
7,158,324	B2	1/2007	Stein et al.	
7,190,288	B2	3/2007	Robinson et al.	
7,190,721	B2	3/2007	Garrett	
7,205,798	B1	4/2007	Agarwal et al.	
7,206,363	B2	4/2007	Hegde et al.	
7,215,716	B1	5/2007	Smith	
7,269,205	B2	9/2007	Wang	
7,467,338	B2	12/2008	Saul	
7,830,854	B1	11/2010	Sarkar et al.	
7,974,230	B1	7/2011	Talley et al.	
8,005,170	B2	8/2011	Lee et al.	
8,059,737	B2	11/2011	Yang	
8,175,186	B1	5/2012	Wiss et al.	
8,199,804	B1	6/2012	Cheong	
8,248,975	B2	8/2012	Fujita et al.	
8,351,536	B2	1/2013	Mazet et al.	
8,422,589	B2	4/2013	Golitschek Edler Von Elbwart et al.	
8,526,523	B1	9/2013	Eliaz	
8,548,072	B1	10/2013	Eliaz	
8,548,089	B2	10/2013	Agazzi et al.	
8,548,097	B1	10/2013	Eliaz	
8,553,821	B1	10/2013	Eliaz	
8,559,494	B1	10/2013	Eliaz	
8,559,496	B1	10/2013	Eliaz	
8,559,498	B1	10/2013	Eliaz	
8,565,363	B1	10/2013	Eliaz	
8,566,687	B1	10/2013	Eliaz	
8,571,131	B1	10/2013	Eliaz	
8,571,146	B1	10/2013	Eliaz	
8,572,458	B1	10/2013	Eliaz	
8,582,637	B1	11/2013	Eliaz	
8,599,914	B1	12/2013	Eliaz	
8,605,832	B1	12/2013	Eliaz	
8,665,941	B1	3/2014	Eliaz	
8,665,992	B1	3/2014	Eliaz	
8,666,000	B2	3/2014	Eliaz	
8,675,769	B1	3/2014	Eliaz	
8,675,782	B2	3/2014	Eliaz	
8,681,889	B2	3/2014	Eliaz	
8,737,458	B2	5/2014	Eliaz	
8,744,003	B2	6/2014	Eliaz	
8,781,008	B2	7/2014	Eliaz	
8,804,879	B1	8/2014	Eliaz	
8,811,548	B2	8/2014	Eliaz	
8,824,572	B2	9/2014	Eliaz	
8,824,599	B1	9/2014	Eliaz	
8,824,611	B2	9/2014	Eliaz	
8,831,124	B2	9/2014	Eliaz	
8,842,778	B2	9/2014	Eliaz	
8,873,612	B1	10/2014	Eliaz	
8,885,698	B2	11/2014	Eliaz	
8,885,786	B2	11/2014	Eliaz	
8,891,701	B1	11/2014	Eliaz	
8,897,387	B1	11/2014	Eliaz	
8,897,405	B2	11/2014	Eliaz	
2001/0008542	A1	7/2001	Wiebke et al.	
2002/0016938	A1	2/2002	Starr	
2002/0123318	A1	9/2002	Lagarrigue	
2002/0150065	A1	10/2002	Ponnekanti	
2002/0150184	A1	10/2002	Hafeez et al.	
2002/0172297	A1	11/2002	Ouchi et al.	
2003/0016741	A1	1/2003	Sasson et al.	
2003/0132814	A1*	7/2003	Nyberg	333/81 R
2003/0135809	A1	7/2003	Kim	
2003/0210352	A1	11/2003	Fitzsimmons et al.	
2004/0009783	A1*	1/2004	Miyoshi	455/522
2004/0037374	A1	2/2004	Gonikberg	
2004/0086276	A1	5/2004	Lenosky	
2004/0120409	A1	6/2004	Yasotharan et al.	
2004/0142666	A1	7/2004	Creigh et al.	
2004/0170228	A1	9/2004	Vadde	
2004/0174937	A1	9/2004	Ungerboeck	
2004/0203458	A1	10/2004	Nigra	
2004/0227570	A1	11/2004	Jackson et al.	
2004/0240578	A1	12/2004	Thesling	
2004/0257955	A1	12/2004	Yamanaka	
2005/0047517	A1	3/2005	Georgios et al.	
2005/0089125	A1*	4/2005	Zhidkov	375/346
2005/0123077	A1	6/2005	Kim	
2005/0135472	A1	6/2005	Higashino	
2005/0163252	A1	7/2005	McCallister	
2005/0220218	A1	10/2005	Jensen et al.	
2005/0265470	A1	12/2005	Kishigami et al.	
2005/0276317	A1	12/2005	Jeong et al.	
2006/0067396	A1	3/2006	Christensen	
2006/0109780	A1	5/2006	Fechtel	
2006/0171489	A1	8/2006	Ghosh et al.	
2006/0239339	A1	10/2006	Brown et al.	
2006/0245765	A1	11/2006	Elahmadi et al.	
2006/0280113	A1	12/2006	Huo	
2007/0092017	A1	4/2007	Abedi	

(56) **References Cited**

U.S. PATENT DOCUMENTS

2007/0098059	A1	5/2007	Ives	
2007/0098090	A1	5/2007	Ma et al.	
2007/0098116	A1	5/2007	Kim et al.	
2007/0110177	A1	5/2007	Molander et al.	
2007/0110191	A1	5/2007	Kim et al.	
2007/0127608	A1	6/2007	Scheim et al.	
2007/0140330	A1	6/2007	Allpress et al.	
2007/0189404	A1	8/2007	Baum et al.	
2007/0213087	A1	9/2007	Laroia et al.	
2007/0230593	A1	10/2007	Eliaz et al.	
2007/0258517	A1	11/2007	Rollings et al.	
2007/0291719	A1	12/2007	Demirhan et al.	
2008/0002789	A1	1/2008	Jao et al.	
2008/0049598	A1	2/2008	Ma et al.	
2008/0080644	A1	4/2008	Batruni	
2008/0130716	A1	6/2008	Cho et al.	
2008/0130788	A1	6/2008	Copeland	
2008/0159377	A1	7/2008	Allpress et al.	
2008/0207143	A1	8/2008	Skarby et al.	
2008/0260985	A1	10/2008	Shirai et al.	
2009/0003425	A1	1/2009	Shen et al.	
2009/0028234	A1	1/2009	Zhu	
2009/0075590	A1	3/2009	Sahinoglu et al.	
2009/0086808	A1	4/2009	Liu et al.	
2009/0122854	A1	5/2009	Zhu et al.	
2009/0185612	A1	7/2009	McKown	
2009/0213908	A1	8/2009	Bottomley	
2009/0245226	A1	10/2009	Robinson	
2009/0290620	A1	11/2009	Tzannes et al.	
2009/0323841	A1	12/2009	Clerckx et al.	
2010/0002692	A1	1/2010	Bims	
2010/0034253	A1	2/2010	Cohen	
2010/0039100	A1	2/2010	Sun et al.	
2010/0062705	A1	3/2010	Rajkotia et al.	
2010/0074349	A1	3/2010	Hyllander et al.	
2010/0166050	A1	7/2010	Aue	
2010/0172309	A1	7/2010	Forenza et al.	
2010/0202505	A1	8/2010	Yu et al.	
2010/0202507	A1	8/2010	Allpress et al.	
2010/0208774	A1	8/2010	Guess et al.	
2010/0208832	A1	8/2010	Lee et al.	
2010/0215107	A1	8/2010	Yang	
2010/0220825	A1	9/2010	Dubuc et al.	
2010/0278288	A1	11/2010	Panicker et al.	
2010/0284481	A1	11/2010	Murakami et al.	
2010/0309796	A1	12/2010	Khayrallah	
2010/0329325	A1	12/2010	Mobin et al.	
2011/0051864	A1	3/2011	Chalia et al.	
2011/0064171	A1	3/2011	Huang et al.	
2011/0069791	A1	3/2011	He	
2011/0074500	A1	3/2011	Bouillet et al.	
2011/0074506	A1	3/2011	Kleider et al.	
2011/0075745	A1	3/2011	Kleider	
2011/0090986	A1	4/2011	Kwon et al.	
2011/0134899	A1	6/2011	Jones, IV et al.	
2011/0150064	A1	6/2011	Kim et al.	
2011/0164492	A1	7/2011	Ma et al.	
2011/0170630	A1	7/2011	Silverman	
2011/0188550	A1	8/2011	Wajcer et al.	
2011/0228869	A1	9/2011	Barsoum et al.	
2011/0243266	A1	10/2011	Roh	
2011/0249709	A1*	10/2011	Shiue et al.	375/219
2011/0275338	A1	11/2011	Seshadri et al.	
2011/0310823	A1	12/2011	Nam et al.	
2011/0310978	A1	12/2011	Wu et al.	
2012/0051464	A1	3/2012	Kamuf et al.	
2012/0106617	A1	5/2012	Jao et al.	
2012/0163489	A1	6/2012	Ramakrishnan	
2012/0177138	A1	7/2012	Chrabieh	
2012/0207248	A1	8/2012	Ahmed et al.	
2013/0028299	A1	1/2013	Tsai	
2013/0044877	A1	2/2013	Liu et al.	
2013/0077563	A1	3/2013	Kim et al.	
2013/0121257	A1	5/2013	He et al.	
2013/0343480	A1	12/2013	Eliaz	
2013/0343487	A1	12/2013	Eliaz	
2014/0036986	A1	2/2014	Eliaz	
2014/0056387	A1	2/2014	Asahina	
2014/0098841	A2	4/2014	Song et al.	
2014/0098907	A1	4/2014	Eliaz	
2014/0098915	A1	4/2014	Eliaz	
2014/0105267	A1	4/2014	Eliaz	
2014/0105268	A1	4/2014	Eliaz	
2014/0105332	A1	4/2014	Eliaz	
2014/0105334	A1	4/2014	Eliaz	
2014/0108892	A1	4/2014	Eliaz	
2014/0133540	A1	5/2014	Eliaz	
2014/0140388	A1	5/2014	Eliaz	
2014/0140446	A1	5/2014	Eliaz	
2014/0146911	A1	5/2014	Eliaz	
2014/0161158	A1	6/2014	Eliaz	
2014/0161170	A1	6/2014	Eliaz	
2014/0198255	A1	7/2014	Kegasawa	

OTHER PUBLICATIONS

Modulation and Coding for Linear Gaussian Channels, G. David Forney, Jr., and Gottfried Ungerboeck, IEEE Transactions of Information Theory, vol. 44, No. 6, Oct. 1998 pp. 2384-2415 (32 pages).

Intuitive Guide to Principles of Communications, www.complextoreal.com, Inter Symbol Interference (ISI) and Root-raised Cosine (RRC) filtering, (2002), pp. 1-23 (23 pages).

Chan, N., "Partial Response Signaling with a Maximum Likelihood Sequence Estimation Receiver" (1980). Open Access Dissertations and Theses. Paper 2855, (123 pages).

The Viterbi Algorithm, Ryan, M.S. and Nudd, G.R., Department of Computer Science, Univ. of Warwick, Coventry, (1993) (17 pages).

R. A. Gibby and J. W. Smith, "Some extensions of Nyquist's telegraph transmission theory," Bell Syst. Tech. J., vol. 44, pp. 1487-1510, Sep. 1965.

J. E. Mazo and H. J. Landau, "On the minimum distance problem for faster-than-Nyquist signaling," IEEE Trans. Inform. Theory, vol. 34, pp. 1420-1427, Nov. 1988.

D. Hajela, "On computing the minimum distance for faster than Nyquist signaling," IEEE Trans. Inform. Theory, vol. 36, pp. 289-295, Mar. 1990.

G. Ungerboeck, "Adaptive maximum-likelihood receiver for carrier modulated data-transmission systems," IEEE Trans. Commun., vol. 22, No. 5, pp. 624-636, May 1974.

G. D. Forney, Jr., "Maximum-likelihood sequence estimation of digital sequences in the presence of intersymbol interference," IEEE Trans. Inform. Theory, vol. 18, No. 2, pp. 363-378, May 1972.

A. Duel-Hallen and C. Heegard, "Delayed decision-feedback sequence estimation," IEEE Trans. Commun., vol. 37, pp. 428-436, May 1989.

M. V. Eyubog •Iu and S. U. Qureshi, "Reduced-state sequence estimation with set partitioning and decision feedback," IEEE Trans. Commun., vol. 36, pp. 13-20, Jan. 1988.

W. H. Gerstacker, F. Obernosterer, R. Meyer, and J. B. Huber, "An efficient method for prefilter computation for reduced-state equalization," Proc. of the 11th IEEE Int. Symp. Personal, Indoor and Mobile Radio Commun. PIMRC, vol. 1, pp. 604-609, London, UK, Sep. 18-21, 2000.

W. H. Gerstacker, F. Obernosterer, R. Meyer, and J. B. Huber, "On prefilter computation for reduced-state equalization," IEEE Trans. Wireless Commun., vol. 1, No. 4, pp. 793-800, Oct. 2002.

Joachim Hagenauer and Peter Hoeher, "A Viterbi algorithm with soft-decision outputs and its applications," in Proc. IEEE Global Telecommunications Conference 1989, Dallas, Texas, pp. 1690-1686,Nov. 1989.

S. Mita, M. Izumita, N. Doi, and Y. Eto, "Automatic equalizer for digital magnetic recording systems" IEEE Trans. Magn., vol. 25, pp. 3672-3674,1987.

E. Biglieri, E. Chiaberto, G. P. Maccone, and E. Viterbo, "Compensation of nonlinearities in high-density magnetic recording channels," IEEE Trans. Magn., vol. 30, pp. 5079-5086, Nov. 1994.

E. Ryan and A. Gutierrez, "Performance of adaptive Volterra equalizers on nonlinear magnetic recording channels," IEEE Trans. Magn., vol. 31, pp. 3054-3056, Nov. 1995.

(56) **References Cited**

OTHER PUBLICATIONS

X. Che, "Nonlinearity measurements and write precompensation studies for a PRML recording channel," IEEE Trans. Magn., vol. 31, pp. 3021-3026, Nov. 1995.

O. E. Agazzi and N. Sheshadri, "On the use of tentative decisions to cancel intersymbol interference and nonlinear distortion (with application to magnetic recording channels)," IEEE Trans. Inform. Theory, vol. 43, pp. 394-408, Mar. 1997.

Miao, George J., Signal Processing for Digital Communications, 2006, Artech House, pp. 375-377.

Xiong, Fuqin. Digital Modulation Techniques, Artech House, 2006, Chapter 9, pp. 447-483.

Faulkner, Michael, "Low-Complex ICI Cancellation for Improving Doppler Performance in OFDM Systems", Center for Telecommunication and Microelectronics, 1-4244-0063-5/06/$2000 (c) 2006 IEEE. (5 pgs).

Stefano Tomasin, et al. "Iterative Interference Cancellation and Channel Estimation for Mobile OFDM", IEEE Transactions on Wireless Communications, vol. 4, No. 1, Jan. 2005, pp. 238-245.

Int'l Search Report and Written Opinion for PCT/IB2013/01866 dated Mar. 21, 2014.

Int'l Search Report and Written Opinion for PCT/IB2013/001923 dated Mar. 21, 2014.

Int'l Search Report and Written Opinion for PCT/IB2013/001878 dated Mar. 21, 2014.

Int'l Search Report and Written Opinion for PCT/IB2013/002383 dated Mar. 21, 2014.

Int'l Search Report and Written Opinion for PCT/IB2013/01860 dated Mar. 21, 2014.

Int'l Search Report and Written Opinion for PCT/IB2013/01970 dated Mar. 27, 2014.

Int'l Search Report and Written Opinion for PCT/IB2013/01930 dated May 15, 2014.

Int'l Search Report and Written Opinion for PCT/IB2013/02081 dated May 22, 2014.

Al-Dhahir, Naofal et al., "MMSE Decision-Feedback Equalizers: Finite-Length Results" IEEE Transactions on Information Theory, vol. 41, No. 4, Jul. 1995.

Cioffi, John M. et al., "MMSE Decision-Feedback Equalizers and Coding—Park I: Equalization Results" IEEE Transactions onCommunications, vol. 43, No. 10, Oct. 1995.

Eyuboglu, M. Vedat et al., "Reduced-State Sequence Estimation with Set Partitioning and Decision Feedback" IEEE Transactions onCommunications, vol. 36, No. 1, Jan. 1988.

* cited by examiner

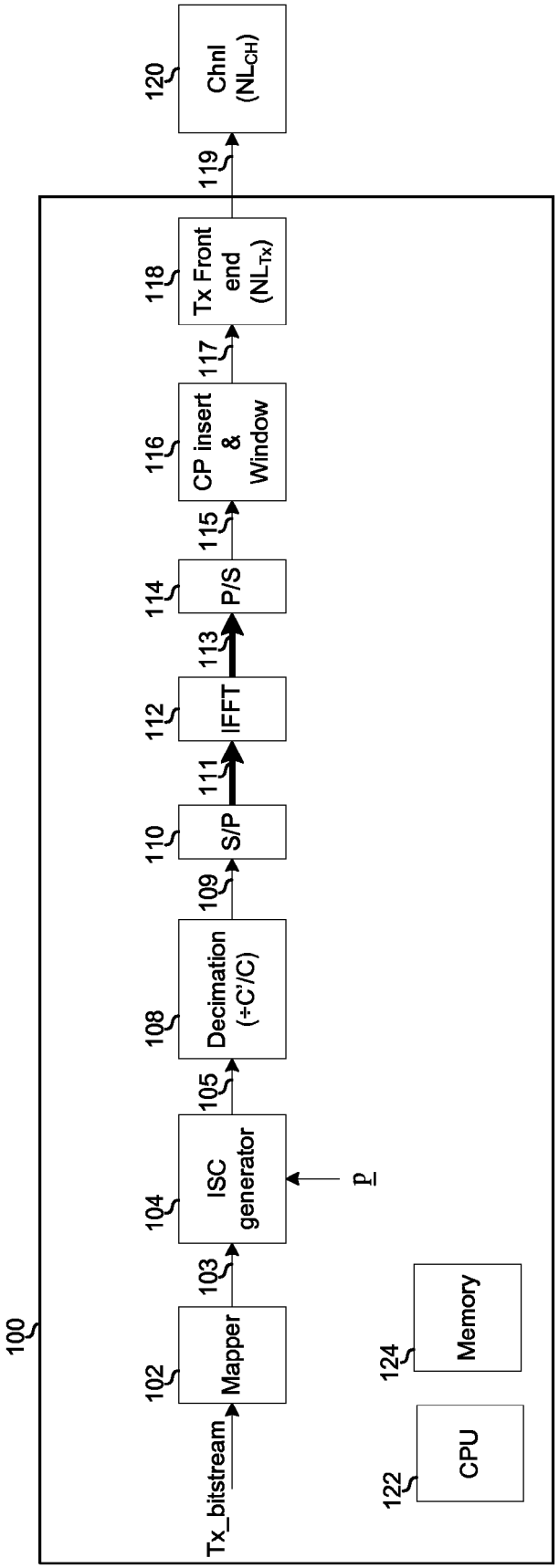
100
Tx_bitstream
102
Mapper
103
104
ISC generator
p
105
108
Decimation (÷C'/C)
109
110
S/P
111
112
IFFT
113
114
P/S
115
116
CP insert & Window
117
118
Tx Front end (NL$_{Tx}$)
119
120
Chnl (NL$_{CH}$)
122
CPU
124
Memory

FIG. 1A

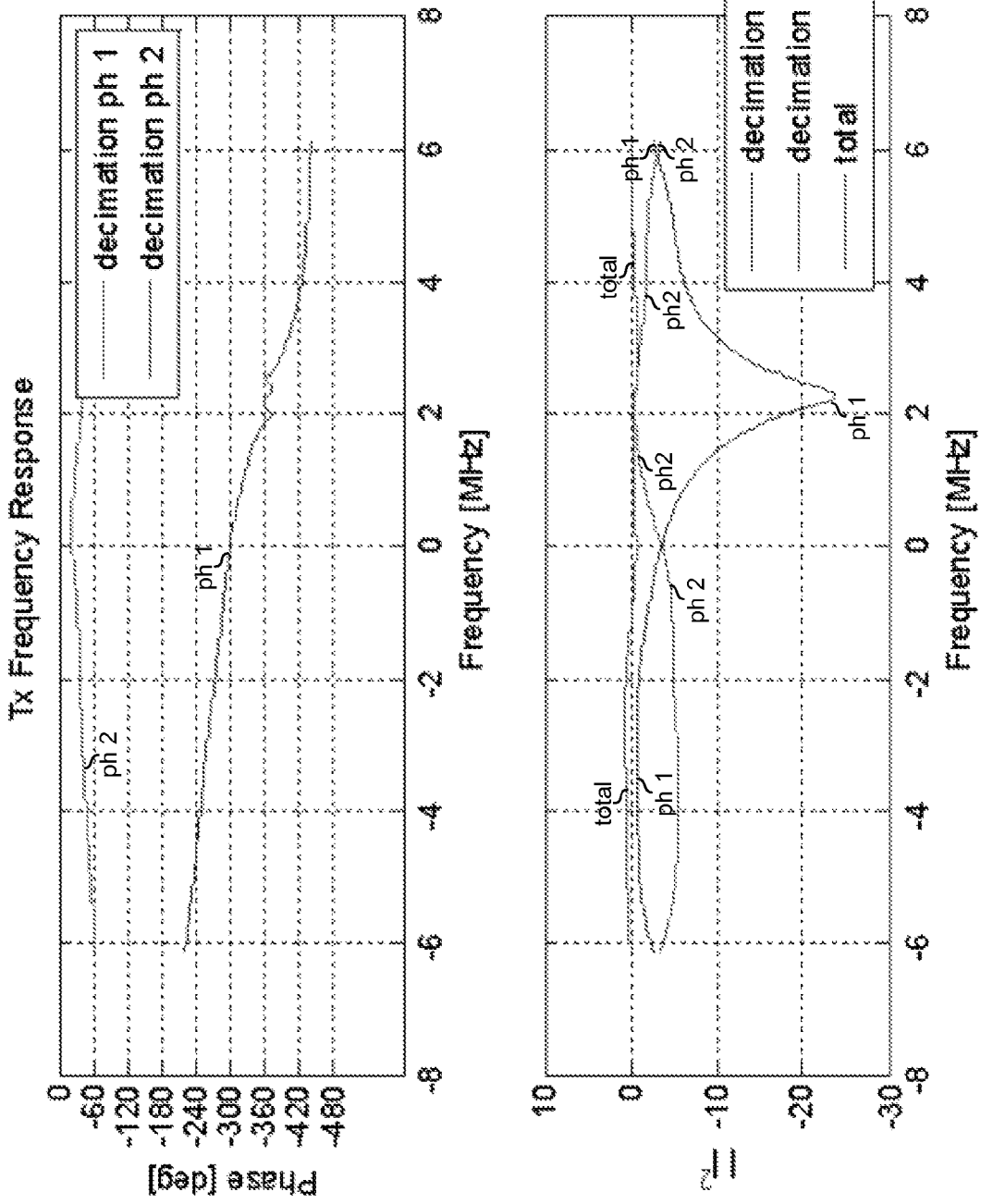
Tx Frequency Response
decimation ph 1
decimation ph 2
total
ph 1
ph 2
Phase [deg]
Frequency [MHz]
0
-60
-120
-180
-240
-300
-360
-420
-480
10
-10
-20
-30
-8
-6
-4
-2
2
4
6
8

FIG. 1B

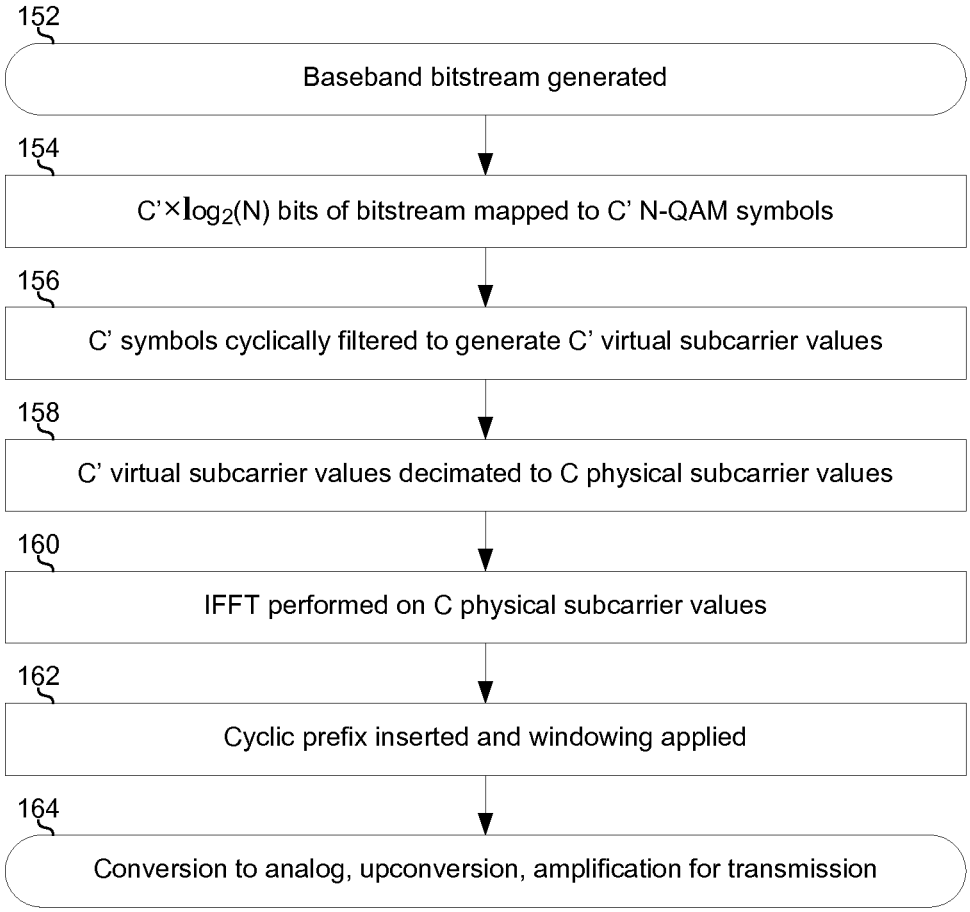
152
Baseband bitstream generated
154
C'×log2(N) bits of bitstream mapped to C' N-QAM symbols
156
C' symbols cyclically filtered to generate C' virtual subcarrier values
158
C' virtual subcarrier values decimated to C physical subcarrier values
160
IFFT performed on C physical subcarrier values
162
Cyclic prefix inserted and windowing applied
164
Conversion to analog, upconversion, amplification for transmission

FIG. 1C

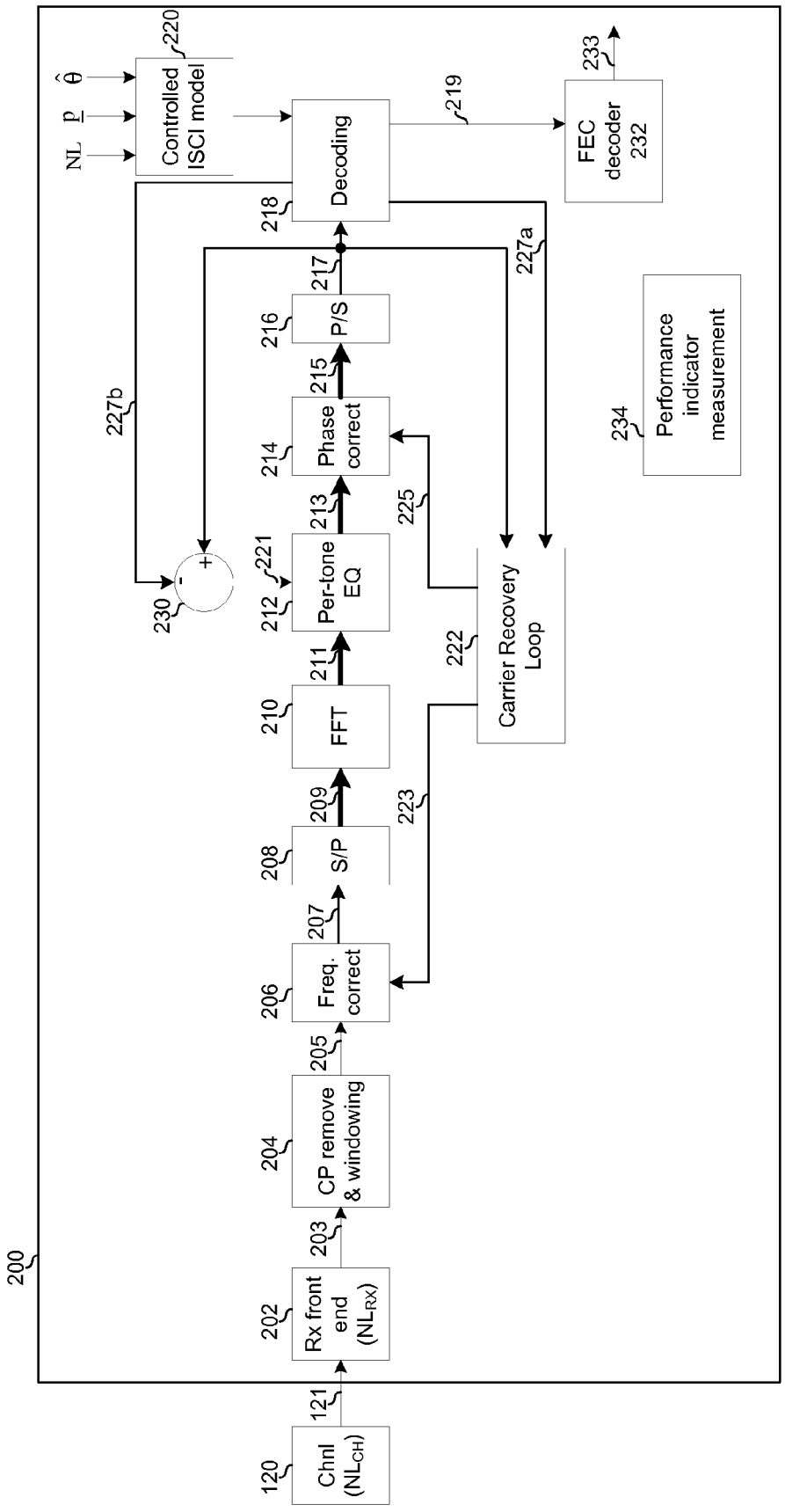
200
120
Chnl (NL_{CH})
121
202
Rx front end (NL_{RX})
203
204
CP remove & windowing
205
206
Freq. correct
207
208
S/P
209
210
FFT
211
212
Per-tone EQ
213
214
Phase correct
215
216
P/S
217
218
Decoding
219
220
Controlled ISCI model
NL
$\underline{p}$
$\hat{\theta}$
222
Carrier Recovery Loop
223
225
227a
227b
230
221
FEC decoder 232
233
234
Performance indicator measurement

FIG. 2A

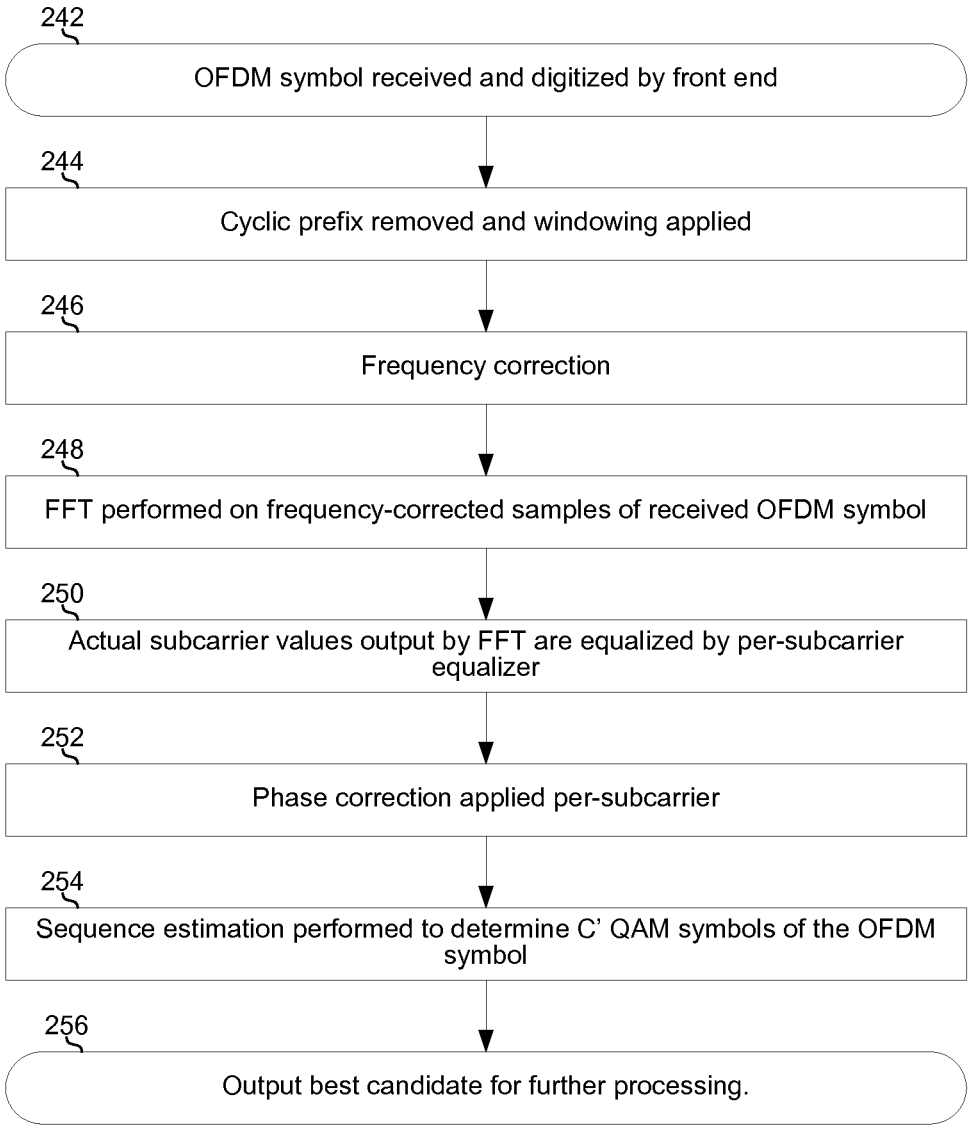
242
OFDM symbol received and digitized by front end
244
Cyclic prefix removed and windowing applied
246
Frequency correction
248
FFT performed on frequency-corrected samples of received OFDM symbol
250
Actual subcarrier values output by FFT are equalized by per-subcarrier equalizer
252
Phase correction applied per-subcarrier
254
Sequence estimation performed to determine C' QAM symbols of the OFDM symbol
256
Output best candidate for further processing.

FIG. 2B

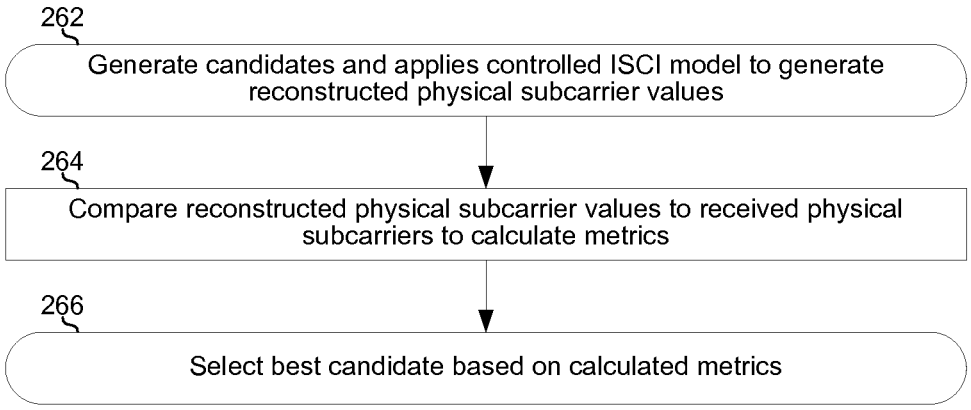
262
Generate candidates and applies controlled ISCI model to generate reconstructed physical subcarrier values
264
Compare reconstructed physical subcarrier values to received physical subcarriers to calculate metrics
266
Select best candidate based on calculated metrics

FIG. 2C

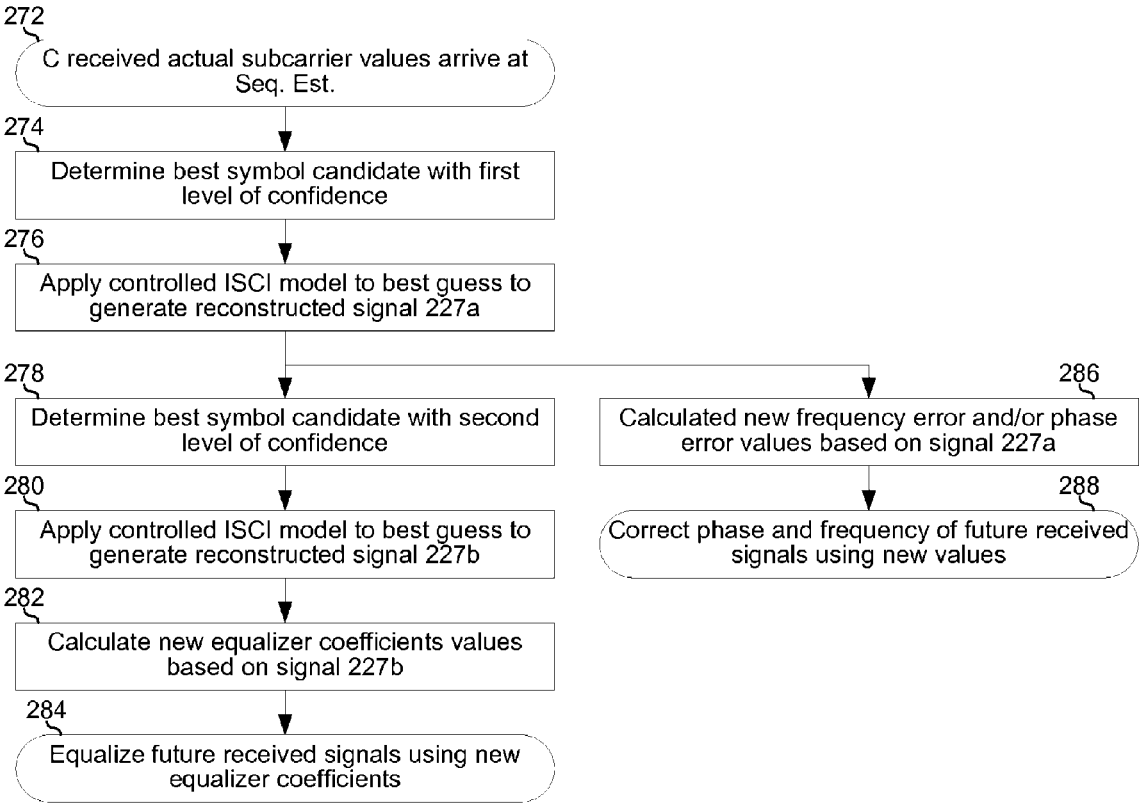
272
C received actual subcarrier values arrive at Seq. Est.
274
Determine best symbol candidate with first level of confidence
276
Apply controlled ISCI model to best guess to generate reconstructed signal 227a
278
Determine best symbol candidate with second level of confidence
280
Apply controlled ISCI model to best guess to generate reconstructed signal 227b
282
Calculate new equalizer coefficients values based on signal 227b
284
Equalize future received signals using new equalizer coefficients
286
Calculated new frequency error and/or phase error values based on signal 227a
288
Correct phase and frequency of future received signals using new values

FIG. 2D

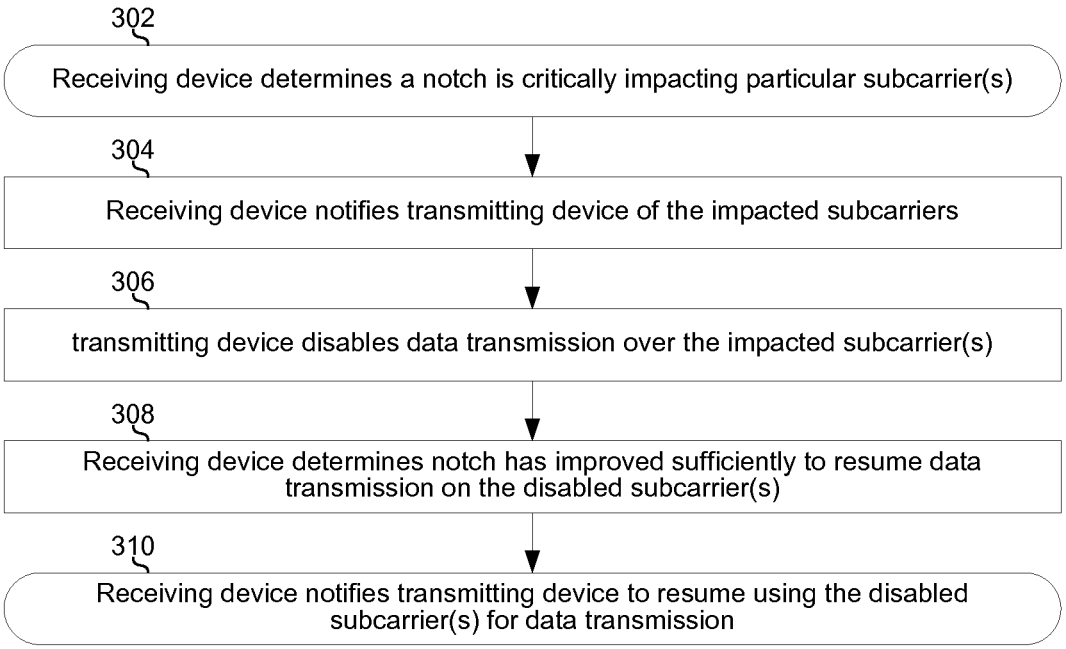
302
Receiving device determines a notch is critically impacting particular subcarrier(s)
304
Receiving device notifies transmitting device of the impacted subcarriers
306
transmitting device disables data transmission over the impacted subcarrier(s)
308
Receiving device determines notch has improved sufficiently to resume data transmission on the disabled subcarrier(s)
310
Receiving device notifies transmitting device to resume using the disabled subcarrier(s) for data transmission

FIG. 3

HIGHLY-SPECTRALLY-EFFICIENT TRANSMISSION USING ORTHOGONAL FREQUENCY DIVISION MULTIPLEXING

CLAIM OF PRIORITY

This patent application is a continuation of Ser. No. 13/921,665 now issued as U.S. Pat. No. 8,781,008, which in turn claims priority to U.S. Provisional Patent Application Ser. No. 61/662,085 titled "Apparatus and Method for Efficient Utilization of Bandwidth" and filed on Jun. 20, 2012, U.S. Provisional Patent Application Ser. No. 61/726,099 titled "Modulation Scheme Based on Partial Response" and filed on Nov. 14, 2012, U.S. Provisional Patent Application Ser. No. 61/729,774 titled "Modulation Scheme Based on Partial Response" and filed on Nov. 26, 2012, U.S. Provisional Patent Application Ser. No. 61/747,132 titled "Modulation Scheme Based on Partial Response" and filed on Dec. 28, 2012, U.S. Provisional Patent Application Ser. No. 61/768,532 titled "High Spectral Efficiency over Non-Linear, AWGN Channels" and filed on Feb. 24, 2013, and U.S. Provisional Patent Application Ser. No. 61/807,813 titled "High Spectral Efficiency over Non-Linear, AWGN Channels" and filed on Apr. 3, 2013, and which is a continuation-in-part of U.S. patent application Ser. No. 13/755,008 titled "Dynamic Filter Adjustment for Highly-Spectrally-Efficient Communications" and filed on Jan. 31, 2013.

Each of the above applications is hereby incorporated herein by reference in its entirety.

INCORPORATIONS BY REFERENCE

This patent application makes reference to:

U.S. patent application Ser. No. 13/754,964, titled "Low-Complexity, Highly-Spectrally-Efficient Communications," and filed on Jan. 31, 2013, now patented as U.S. Pat. No. 8,582,637;

U.S. patent application Ser. No. 13/754,998, titled "Design and Optimization of Partial Response Pulse Shape Filter," and filed on Jan. 31, 2013;

U.S. patent application Ser. No. 13/755,001 , titled "Constellation Map Optimization for Highly Spectrally Efficient Communications," and filed on Jan. 31, 2013, now patented as U.S. Pat. No. 8,675,769;

U.S. patent application Ser. No. 13/755,008 , titled "Dynamic Filter Adjustment for Highly-Spectrally-Efficient Communications," and filed on Jan. 31, 2013, now patented as U.S. Pat. No. 8,571,131;

U.S. patent application Ser. No. 13/755,011 , titled "Timing Synchronization for Reception of Highly-Spectrally-Efficient Communications," and filed on Jan. 31, 2013, now patented as U.S. Pat. No. 8,559,494;

U.S. patent application Ser. No. 13/755,014 , titled "Signal Reception Using Non-Linearity-Compensated, Partial Response Feedback," and filed on Jan. 31, 2013, now patented as U.S. Pat. No. 8,559,496;

U.S. patent application Ser. No. 13/755,018 , titled "Feed Forward Equalization for Highly-Spectrally-Efficient Communications," and filed on Jan. 31, 2013, now patented as U.S. Pat. No. 8,599,914;

U.S. patent application Ser. No. 13/755,021 , titled "Decision Feedback Equalizer for Highly Spectrally Efficient Communications," and filed on Jan. 31, 2013, now patented as U.S. Pat. No. 8,665,941;

U.S. patent application Ser. No. 13/755,025, titled "Decision Feedback Equalizer with Multiple Cores for Highly-Spectrally-Efficient Communications," and filed on Jan. 31, 2013;

U.S. patent application Ser. No. 13/755,026 , titled "Decision Feedback Equalizer Utilizing Symbol Error Rate Biased Adaptation Function for Highly Spectrally Efficient Communications," and filed on Jan. 31, 2013, now patented as U.S. Pat. No. 8,559,498;

U.S. patent application Ser. No. 13/755,028 , titled "Coarse Phase Estimation For Highly-Spectrally-Efficient Communications," and filed on Jan. 31, 2013, now patented as U.S. Pat. No. 8,548,097;

U.S. patent application Ser. No. 13/755,039 , titled "Fine Phase Estimation for Highly Spectrally Efficient Communications," and filed on Jan. 31, 2013, now patented as U.S. Pat. No. 8,565,363;

U.S. patent application Ser. No. 13/755,972 , titled "Multi-Mode Transmitter for Highly-Spectrally-Efficient Communications," and filed on Jan. 31, 2013, now patented as U.S. Pat. No. 8,744,003;

U.S. patent application Ser. No. 13/755,043 , titled "Joint Sequence Estimation of Symbol and Phase With High Tolerance Of Nonlinearity," and filed on Jan. 31, 2013, now patented as U.S. Pat. No. 8,605,832;

U.S. patent application Ser. No. 13/755,050 , titled "Adaptive Non-Linear Model for Highly-Spectrally-Efficient Communications," and filed on Jan. 31, 2013, now patented as U.S. Pat. No. 8,553,821;

U.S. patent application Ser. No. 13/755,052, titled "Pilot Symbol-Aided Sequence Estimation for Highly-Spectrally-Efficient Communications," and filed on Jan. 31, 2013;

U.S. patent application Ser. No. 13/755,054 , titled "Method and System for Corrupt Symbol Handling for Providing High Reliability Sequences," and filed on Jan. 31, 2013, now patented as U.S. Pat. No. 8,571,146;

U.S. patent application Ser. No. 13/755,060 , titled "Method and System for Forward Error Correction Decoding with Parity Check for Use in Low Complexity Highly-spectrally-efficient Communications," and filed on Jan. 31, 2013, now patented as U.S. Pat. No. 8,566,687;

U.S. patent application Ser. No. 13/755,061, titled "Method and System for Quality of Service (QoS) Awareness in a Single Channel Communication System," and filed on Jan. 31, 2013;

U.S. patent application Ser. No. 13/756,079 , titled "Pilot Symbol Generation for Highly-Spectrally-Efficient Communications," and filed on Jan. 31, 2013, now patented as U.S. Pat. No. 8,665,992;

U.S. patent application Ser. No. 13/755,065, titled "Timing Pilot Generation for Highly-Spectrally-Efficient Communications," and filed on Jan. 31, 2013, now patented as U.S. Pat. No. 8,548,072;

U.S. patent application Ser. No. 13/756,010, titled "Multi-Mode Receiver for Highly-Spectrally-Efficient Communications," and filed on Jan. 31, 2013;

U.S. patent application Ser. No. 13/755,068, titled "Forward Error Correction with Parity Check Encoding for use in Low Complexity Highly-spectrally-efficient Communications," and filed on Jan. 31, 2013, now patented as U.S. Pat. No. 8,572,458;

U.S. patent application Ser. No. 13/756,469, titled "Highly-Spectrally-Efficient Receiver," and filed on Jan. 31, 2013, now patented as U.S. Pat. No. 8,526,523;

U.S. patent application Ser. No. 13/921,665, titled "Highly-Spectrally-Efficient Reception Using Orthogonal Fre-

quency Division Multiplexing," and filed on Jun. 19, 2013, now patented as U.S. Pat. No. 8,781,008;

U.S. patent application Ser. No. 13/921,749, titled "Multi-Mode Orthogonal Frequency Division Multiplexing Transmitter for Highly-Spectrally-Efficient Communications," and filed on Jun. 19, 2013; and

U.S. patent application Ser. No. 13/921,813, titled "Multi-Mode Orthogonal Frequency Division Multiplexing Receiver for Highly-Spectrally-Efficient Communications," and filed on Jun. 19, 2013 now patented as U.S. Pat. No. 8,681,889.

Each of the above applications is hereby incorporated herein by reference in its entirety.

TECHNICAL FIELD

Aspects of the present application relate to electronic communications.

BACKGROUND

Existing communications methods and systems are overly power hungry and/or spectrally inefficient. Further limitations and disadvantages of conventional and traditional approaches will become apparent to one of skill in the art, through comparison of such approaches with some aspects of the present method and system set forth in the remainder of this disclosure with reference to the drawings.

BRIEF SUMMARY

Methods and systems are provided for highly-spectrally-efficient communications using orthogonal frequency division multiplexing, substantially as illustrated by and/or described in connection with at least one of the figures, as set forth more completely in the claims.

BRIEF DESCRIPTION OF THE DRAWINGS

FIG. **1**A is a diagram of an example OFDM transmitter.

FIG. **1**B depicts simulation results of an example cyclic filter for a highly-spectrally-efficient OFDM transmitter.

FIG. **1**C depicts a flowchart describing operation of an example implementation of a highly-spectrally-efficient OFDM transmitter.

FIG. **2**A is a diagram of an example OFDM receiver.

FIGS. **2**B and **2**C depict a flowchart describing operation of an example implementation of a highly-spectrally-efficient OFDM receiver.

FIG. **2**D depicts a flowchart describing operation of an example decoding circuit of a highly-spectrally-efficient OFDM receiver.

FIG. **3** is a flowchart describing a process for mitigating the effects of frequency-selective fading in highly-spectrally-efficient OFDM communication system.

DETAILED DESCRIPTION

As utilized herein the terms "circuits" and "circuitry" refer to physical electronic components (i.e. hardware) and any software and/or firmware ("code") which may configure the hardware, be executed by the hardware, and or otherwise be associated with the hardware. As used herein, for example, a particular processor and memory may comprise a first "circuit" when executing a first one or more lines of code and may comprise a second "circuit" when executing a second one or more lines of code. As utilized herein, "and/or" means any one or more of the items in the list joined by "and/or". As an example, "x and/or y" means any element of the three-element set {(x), (y), (x, y)}. As another example, "x, y, and/or z" means any element of the seven-element set {(x), (y), (z), (x, y), (x, z), (y, z), (x, y, z)}. As utilized herein, the term "exemplary" means serving as a non-limiting example, instance, or illustration. As utilized herein, the terms "e.g.," and "for example" set off lists of one or more non-limiting examples, instances, or illustrations. As utilized herein, circuitry is "operable" to perform a function whenever the circuitry comprises the necessary hardware and code (if any is necessary) to perform the function, regardless of whether performance of the function is disabled, or not enabled, by some user-configurable setting.

Orthogonal Frequency Division Multiplexing (OFDM) has gained traction in recent years in high-capacity wireless and wireline communication systems such as WiFi (IEEE Std 802.11n/ac), 3GPP-LTE, and G.hn. One advantage of OFDM is that it can reduce the need for complicated equalization over frequency selective channels. It is particularly powerful in combination with multiple independent spatial streams and multiple antennas, Multiple Input Multiple Output (MIMO) systems. One advantage of OFDM is that it can reduce or eliminate the need for complicated equalization over frequency selective channels. Conventional MIMO-OFDM solutions are based on suboptimal Zero Forcing, SIC (Successive Interference Cancellation), and minimum mean square error (MMSE) receivers. These detection algorithms are significantly inferior to maximum likelihood (ML) and near-ML receivers. Lately, in emerging standards, constellation size continues to increase (256-QAM, 1024-QAM, and so on). The associated ML state space of such solutions is N^{SS}, where N and SS stand for the constellation size and total number of MIMO spatial streams, respectively. Consequently, aspects of this disclosure pertain to reduced state/complexity ML decoders that achieve high performance.

Example implementations of the present disclosure may use relatively small constellations with partial response signaling that occupies around half the bandwidth of "ISI-free" or "full response" signaling. Thus, the ML state space is reduced significantly and cost effectiveness of reduced complexity ML detection is correspondingly improved. Additionally, aspects of this disclosure support detection in the presence of phase noise and non-linear distortion without the need of pilot symbols that reduce capacity and spectral efficiency. The spectral compression also provides multidimensional signal representation that improves performance in an AWGN environment as compared to conventional two-dimensional QAM systems. In accordance with an implementation of this disclosure, transmitter shaping filtering may be applied in the frequency domain in order to preserve the independency of the OFDM symbols.

FIG. **1**A is a diagram of an example OFDM transmitter. The example transmitter **100** comprises a symbol mapper circuit **102**, an inter-symbol correlation (ISC) generation circuit **104**, a decimation circuit **108**, a serial-to-parallel circuit **108**, an inverse fast Fourier transform (IFFT) circuit **112**, a parallel-to-serial circuit **114**, a cyclic prefix and windowing circuit **116**, and a transmit front-end circuit **118**. In the example implementation shown, the transmitter transmits into a channel **120**.

The symbol mapper circuit **102**, may be operable to map, according to a selected modulation scheme, bits of a bitstream to be transmitted ("Tx_bitstream") to symbols. For example, for a quadrature amplitude modulation (QAM) scheme having a symbol alphabet of N (N-QAM), the mapper may map each $\text{Log}_2(N)$ bits of the Tx_bitstream to a single symbol

represented as a complex number and/or as in-phase (I) and quadrature-phase (Q) components. Although N-QAM is used for illustration in this disclosure, aspects of this disclosure are applicable to any modulation scheme (e.g., pulse amplitude modulation (PAM), amplitude shift keying (ASK), phase shift keying (PSK), frequency shift keying (FSK), etc.). Additionally, points of the N-QAM constellation may be regularly spaced ("on-grid") or irregularly spaced ("off-grid"). Furthermore, the symbol constellation used by the mapper **102** may be optimized for best bit-error rate (BER) performance (or adjusted to achieve a target BER) that is related to log-likelihood ratio (LLR) and to optimizing mean mutual information bit (MMIB) (or achieving a target MMIB). The Tx_bitstream may, for example, be the result of bits of data passing through a forward error correction (FEC) encoder and/or an interleaver. Additionally, or alternatively, the symbols out of the mapper **102** may pass through an interleaver.

The ISC generation circuit **104** may be operable to filter the symbols output by the mapper **102** to generate C' virtual subcarrier values (the terminology "virtual subcarrier" is explained below) having a significant, controlled amount inter-symbol correlation among symbols to be output on different subcarriers (i.e., any particular one of the C' virtual subcarrier values may be correlated with a plurality of the C' symbols output by mapper **102**). In other words, the inter-symbol correlation introduced by the ISC generation circuit may be correlation between symbols to be output on different subcarriers. In an example implementation, the ISC generation circuit **104** may be a cyclic filter.

The response of the ISC generation circuit **104** may be determined by a plurality of coefficients, denoted $\underline{p}$ (where underlining indicates a vector), which may be, for example, stored in memory **124**. In an example implementation, the ISC generation circuit **104** may perform a cyclic (or, equivalently, "circular") convolution on sets of C' symbols from the mapper **102** to generate sets of C' virtual subcarrier values conveyed as signal **105**. In such an implementation, the ISC generation circuit **104** may thus be described as a circulant matrix that multiplies an input vector of C' symbols by a C'×C' matrix, where each row i+1 of the matrix may be a circularly shifted version of row i of the matrix, i being an integer from 1 to C'. For example, for C'=4 (an arbitrary value chosen for illustration only) and $\underline{p}$=[p1 p2 p3 p4], the matrix may be as follows:

$$\begin{bmatrix} p1 & p2 & p3 & p4 \\ p4 & p1 & p2 & p3 \\ p3 & p4 & p1 & p2 \\ p2 & p3 & p4 & p1 \end{bmatrix}$$

In another example, the length of p may be less than C', and zero padding may be used to fill the rows and/or columns to length C' and/or pad the rows and/or columns. For example, C' may be equal to 6 and the matrix above (with $\underline{p}$ having four elements) may be padded to create a six element vector $\underline{p}_Z$=[p1 p2 p3 p4 0 0] and then $\underline{p}_Z$ may be used to generate a 6 by 6 matrix in the same way that $\underline{p}$ was used to generate the 4 by 4 matrix. As another example, only the rows may be padded such that the result is a C'×LP matrix, where LP is the length of $\underline{p}$ (e.g., a 4×6 matrix in the above example). As another example, only the columns may be padded such that the result is a LP×C' matrix, where LP is the length of $\underline{p}$ (e.g., a 6×4 matrix in the above example).

The decimation circuit **108** may be operable to decimate groups of C' virtual subcarrier values down to C transmitted physical subcarrier values (the term "physical subcarrier" is explained below). Accordingly, the decimation circuit **108** may be operable to perform downsampling and/or upsampling. The decimation factor may be an integer or a fraction. The output of the decimator **108** hence comprises C physical subcarrier values per OFDM symbol. The decimation may introduce significant aliasing in case that the ISC generation circuit **104** does not confine the spectrum below the Nyquist frequency of the decimation. However, in example implementations of this disclosure, such aliasing is allowed and actually improves performance because it provides an additional degree of freedom. The C physical subcarrier values may be communicated using C of C+Δ total subcarriers of the channel **120**. Δ may correspond to the number of OFDM subcarriers on the channel **120** that are not used for transmitting data. For example, data may not be transmitted a center subcarrier in order to reduce DC offset issues. As another example, one or more subcarriers may be used as pilots to support phase and frequency error corrections at the receiver. Additionally, zero subcarrier padding may be used to increase the sampling rate that separates the sampling replicas and allow the use of low complexity analog circuitry. The C+Δ subcarriers of channel **120** may be spaced at approximately (e.g., within circuit tolerances) BW/(C+Δ) (according to the Nyquist criterion) and with effective OFDM symbol duration of less than or equal to (C+Δ)/BW (according to the Nyquist criterion). Aspects of the invention may, however, enable the receiver to recover the original C' symbols from the received OFDM symbol (Thus the reason for referring to C' as the number of "virtual subcarriers"). This delivery of C' symbols using C effective subcarriers of bandwidth BW/(C+Δ), and OFDM symbol timing of less than or equal to (C+Δ)/BW thus corresponds to a bandwidth reduction of (C'+Δ)/(C+Δ) or, equivalently, a symbol rate increase of C'/C over conventional OFDM systems (assuming the same number, Δ, of unused subcarriers in the conventional system).

To reduce complexity, in an example implementation, the functionalities of **104** and **108** may be merged by calculating only a subset (C_S) of the C physical subcarriers subset from C' by taking out the rows of the matrix that are related to the decimated virtual subcarriers of the ISC generating, C'×C' matrix. For example, decimation of factor of 2 may be achieved by eliminating the even column vectors of the C'×C' matrix described in paragraph [0021] (assuming, for purposes of this example, that the information symbol vector (length of C') is a row vector that left multiplies the matrix).

Generally speaking, in an example implementation wherein the circuit **104** is a cyclic filter, methods and systems of designing the ISC generation circuit **104** may be similar to methods and systems described in U.S. patent application Ser. No. 13/754,998 titled "Design and Optimization of Partial Response Pulse Shape Filter," which is incorporated by reference above. Similar to the design of the filter(s) in the single-carrier case described in U.S. patent application Ser. No. 13/754,998, the design of a cyclic filter implementation of the circuit **104** may be based on using the symbol error rate (SER) union bound as a cost function and may aim to maximize the Euclidean distance associated with one or more identified error patterns. Using a shaping filter characterized by the coefficients $\underline{p}$, the distance induced by error pattern $\underline{\epsilon}$ may be expressed as:

$$\delta^2(\underline{\epsilon},\underline{p})=\Sigma_n|\Sigma_k p_{[n-k]}\epsilon_{[k]}|^2=\Sigma_k\Sigma_l\epsilon_{[k]}\epsilon_{[l]}{}^*\Sigma_n p_{[n-k]}p_{[n-l]}{}^* \quad \text{Eq. 1A}$$

Assuming, for purposes of illustration, a spectral compression factor 2, then, after decimation by 2, EQ. 1A becomes:

$$\delta_2{}^2(\underline{\epsilon},\underline{p})=\Sigma_n|\Sigma_k p_{[2n-k]}\epsilon_{[k]}|^2=\Sigma_n|\Sigma_k\epsilon_{[2n-2k]}p_{[2k]}+\Sigma_k\epsilon_{[2n-2k+1]}p_{[2k-1]}|^2 \quad \text{Eq. 1B}$$

Where the right-hand-side summation relates to odd-indexed symbols and the left-hand-side summation relates to even-indexed symbols. Eq. 1B may then be rewritten as:

$$\delta_2^2(\epsilon, \underline{p}) = \sum_n \left[\sum_k \sum_m \epsilon_{[2k]} \epsilon^*_{[2m]} p_{[2n-2k]} p^*_{[2n-2m]} + \sum_k \sum_m \epsilon_{[2k-1]} \epsilon^*_{[2m-1]} p_{[2n-2k+1]} p^*_{[2n-2m+1]} + 2 \cdot \mathrm{Real}\left\{ \sum_k \sum_m \epsilon_{[2k]} \epsilon^*_{[2m-1]} p_{[2n-2k]} p^*_{[2n-2m+1]} \right\} \right] \quad \text{Eq. 1C}$$

In Eq. 1C, the first and second summation terms are associated with the distance of the even-indexed and odd-indexed virtual subcarriers respectively. Accordingly, one goal in designing a cyclic filter implementation of ISC generation circuit **104** may be to maximize the first and second terms of Eq. 1C. The third term takes on both positive and negative values depending on the error pattern. In general, this term will reduce the minimum distance related to the most-probable error patterns. Accordingly, one goal in designing a cyclic filter implementation of ISC generation circuit **104** may be to minimize the third term of Eq. 1C (i.e., minimizing cross-correlation between even and odd virtual subcarriers). Additionally or alternatively, a cyclic filter implementation of ISC generation circuit **104** may be designed such that the first and second terms should have similar levels, which may correspond to even-indexed and odd-indexed symbol sequences have comparable distances (i.e., seeking energy balance between even-indexed and odd-indexed virtual subcarriers).

In presence of frequency-selective fading channel, the inter-subcarrier correlation created by **104** (by filtering or by matrix multiplication, for example) may be used to overcome the frequency-selective fading and to improve detection performance at the receiver. The processing of inter-subcarrier correlation may be perceived as "analog interleaving" over the frequency domain that spreads each of the C' information symbols over a plurality of frequency subcarriers. As a result of this "analog interleaving," a notch in one of the subcarriers will have a relatively low impact on detection, assuming that rest of subcarriers that are carrying that information symbol are received with sufficiently-high SNR.

In case of frequency selective fading channel, feedback from the receiving device may be used to dynamically adapt transmission properties. An example process for such dynamic adaption is shown in FIG. **3**.

In block **302** frequency selective fading is causing a significant notch that is critically impacting one or more subcarriers. For example, the notch may be reducing the received SNR of the subcarrier(s) below a certain level (e.g., a level that is predetermined and/or algorithmically controlled during run time).

In block **304**, an identification of such impacted subcarrier(s) may be sent from the receiving device to the transmitting device (e.g., over a control channel).

In block **306**, in response to receiving the indication sent in block **304**, the transmitting device disables transmission of data over the impacted subcarrier(s). The transmitting device may disable transmission of data over the impacted subcarrier(s) by, for example, reconfiguring the mapper **102** (e.g., changing the value of C' and/or configuring the mapper **102** to insert pilot symbols between data symbols), changing p, reconfiguring the decimation circuit **108** (e.g., changing the value of C), and/or reconfiguring the mapping performed by the serial-to-parallel circuit **110**.

In block **308**, the receiving device may determine that data transmission on the disabled subcarriers should resume.

In block **310**, the instruction to resume data transmission on the disabled subcarrier(s) may be sent (e.g., via a control channel). In an example implementation, such a determination may be made by monitoring pilot signal(s) that the transmitting device transmits on the disabled subcarrier(s). For example, the receiving device may monitor a characteristic (e.g., SNR) of the pilot signal(s) and determine to resume use of the subcarriers(s) upon a significant and/or sustained change in the characteristic (e.g., upon SNR of the pilot signal(s) increasing above a determined threshold for a determined amount of time. In an example implementation, the determination to resume data transmission on the disabled subcarrier(s) may be based on the one or more characteristics of subcarriers adjacent to the disabled subcarrier(s). For example, while subcarrier N is disabled, the receiving device may monitor SNR of adjacent subcarriers N−1 and/or N+1, and may decide enable subcarrier N in response to a significant and/or sustained increase in the SNR of subcarrier(s) N−1 and/or N+1. The first example above for SNR estimation of disabled subcarrier(s) which is based on pilots, may be more accurate than the second example which is based on SNR estimation using adjacent subcarriers. However, the second example does not "waste" power on pilot subcarrier(s) transmission thus may provide higher power for the information (modulated) subcarriers assuming that the transmitted power is fixed. The relative increased power of the modulated subcarriers may improve decoding performance (e.g., SER, BER, packet error rate).

Similarly, feedback from the receiving device (e.g., in the form of subcarrier SNR measurements) may be used to adapt the ISC generation circuit **104** and/or decimation circuit **108**. Such adaptation may, for example, give relatively-high-SNR subcarriers relatively-high coefficients and relatively-low-SNR subcarriers relatively-low coefficients. Such adaptation of coefficients may be used to optimize communication capacity (or to achieve a target communication capacity) between the transmitting device and the receiving device. The control channel latency and adaptation rate may be controlled to be fast enough to accommodate channel coherence time.

Returning to FIG. **1**B, additional, or alternative, design goals for the circuit **104** may stem from a desire to reduce complexity of the sequence estimation in the receiver. As an example, one design goal may be, as described in U.S. patent application Ser. No. 13/754,998, maximizing the magnitude of coefficients of "early" (or low-indexed) taps of a cyclic filter implementation of circuit **104**. As another example, one design goal may be, as described in U.S. patent application Ser. No. 13/754,998, minimizing the cumulative power of the "late" (or high-indexed) taps of a cyclic filter implementation of circuit **104**.

As shown by the example simulation results in FIG. **1**B (compression factor=2 used for purposes of illustration), a complex-valued shaping filter can exploit the full spectrum and make the even-indexed ("ph 1") and odd-indexed responses ("ph 2") substantially orthogonal by using disjoint parts of the spectrum. FIG. **1**B shows an example of the frequency response of the even-indexed and odd-indexed coefficients of a cyclic filter implementation of circuit **104** that was designed in accordance with this disclosure. Also, shown in the lower portion of FIG. **1**B is the total/combined even and odd response, which, as can be seen, is substantially flat.

Returning to FIG. **1**A, the serial-to-parallel circuit **110** may be operable to convert C physical subcarrier values conveyed serially as signal **109** to C physical subcarrier values input conveyed in parallels as signals **111**.

In an example implementation, the subcarrier values output by the decimation circuit **108** may be interleaved prior to being input to the circuit **112** and/or the circuit **110** may perform interleaving of the inputted subcarrier values. This interleaver may be operable to improve the tolerance to frequency selective fading caused by multipath that may impose wide notch that spans over several subcarriers. In this case the interleaver may be used to "spread" the notch over non-consecutive (interleaved) subcarriers and therefore reduce the impact of the notch on decoding performance.

Each of the signals **103**, **105**, **109**, and **111** may be frequency-domain signals. The inverse fast Fourier transform (IFFT) circuit **112** may be operable to convert the frequency-domain samples of signals **111** to time-domain samples of signals **113**.

The parallel-to-serial circuit **114** may be operable to convert the parallel signals **113** to a serial signal **115**.

The circuit **116** may be operable to process the signal **115** to generate the signal **117**. The processing may include, for example, insertion of a cyclic prefix. Additionally, or alternatively, the processing may include application of a windowing function to compensate for artifacts that may result when a receiver of the transmitted signal uses the FFT to recover information carried in the transmitted signal. Windowing applied the in transmitter **100** may be instead of, or in addition to, windowing applied in a receiver.

The transmitter front-end **118** may be operable to convert the signal **117** to an analog representation, upconvert the resulting analog signal, and amplify the upconverted signal to generate the signal **119** that is transmitted into the channel **120**. Thus, the transmitter front-end **118** may comprise, for example, a digital-to-analog converter (DAC), mixer, and/or power amplifier. The front-end **118** may introduce non-linear distortion and/or phase noise (and/or other non-idealities) to the signal **117**. The non-linearity of the circuit **118** may be represented as NL_{Tx} which may be, for example, a polynomial, or an exponential (e.g., Rapp model). The non-linearity may incorporate memory (e.g., Voltera series). In an example implementation, the transmitter **100** may be operable to transmit its settings that relate to the nonlinear distortion inflicted on transmitted signals by the front-end **118**. Such transmitted information may enable a receiver to select an appropriate nonlinear distortion model and associated parameters to apply (as described below).

The channel **120** may comprise a wired, wireless, and/or optical communication medium. The signal **119** may propagate through the channel **120** and arrive at a receiver such as the receiver described below with respect to FIG. **2**A.

In various example embodiments, subcarrier-dependent bit-loading and time-varying bit-loading may also be used.

FIG. **1**C depicts a flowchart describing operation of an example implementation of a highly-spectrally-efficient OFDM transmitter. The process begins with block **152** in which a baseband bitstream is generated (e.g., by an application running on a smartphone, tablet computer, laptop computer, or other computing device).

In block **154**, the baseband bitstream is mapped according to a symbol constellation. In the example implementation depicted, C' (an integer) sets of log 2(N) bits of the baseband bitstream are mapped to C' N-QAM symbols.

In block **156**, the C' symbols are cyclically convolved, using a filter designed as described above with reference to FIG. **1**A, to generate C' virtual subcarrier values having a significant, controlled amount of inter-symbol correlation among symbols to be output on different subcarriers.

In block **158**, the C' virtual subcarrier values output by the ISC generation circuit **104** may be decimated down to C physical subcarrier values, each of which is to be transmitted over a respective one of the C+Δ OFDM subcarriers of the channel **120**. In an example implementation, the decimation may be by a factor of between approximately 1.25 and 3.

In block **160**, the C physical subcarrier values are input to the IFFT and a corresponding C+Δ time-domain values are output for transmission over C+Δ subcarriers of the channel **120**.

In block **162**, a cyclic prefix may be appended to the C time domain samples resulting from block **160**. A windowing function may also be applied to the samples after appending the cyclic prefix.

In block **164** the samples resulting from block **162** may be converted to analog, upconverted to RF, amplified, and transmitted into the channel **120** during a OFDM symbol period that is approximately (e.g., within circuit tolerances) (C+Δ)/BW.

FIG. **2**A is a diagram of an example OFDM receiver. The example receiver **200** comprises a front-end **202**, a cyclic prefix and windowing circuit **204**, a serial-to-parallel conversion circuit **208**, a frequency correction circuit **206**, a fast Fourier transform (FFT) circuit **210**, a per-tone equalizer **212**, a phase correction circuit **214**, a parallel-to-serial conversion circuit **216**, a decoding circuit **218**, a controlled combined inter-symbol correlation (ISC) and/or inter-subcarrier interference (ICI) model (Controlled ISCI Model) circuit **220**, a carrier recovery loop circuit **222**, a FEC decoder circuit **232**, and a performance indicator measurement circuit **234**.

The receiver front-end **202** may be operable to amplify, downconvert, and/or digitize the signal **121** to generate the signal **203**. Thus, the receiver front-end **202** may comprise, for example, a low-noise amplifier, a mixer, and/or an analog-to-digital converter. The front-end **202** may, for example, sample the received signal **121** at least C+Δ times per OFDM symbol period. Due to non-idealities, the receiver front-end **202** may introduce non-linear distortion and/or phase noise to the signal **203**. The non-linearity of the front end **202** may be represented as NL_{Rx} which may be, for example, a polynomial, or an exponential (e.g., Rapp model). The non-linearity may incorporate memory (e.g., Voltera series).

The circuit **204** may be operable to process the signal **203** to generate the signal **205**. The processing may include, for example, removal of a cyclic prefix. Additionally, or alternatively, the processing may include application of a windowing function to compensate for artifacts that may result from use of an FFT on a signal that is not periodic over the FFT window. Windowing applied in the transmitter **100** may be instead of, or in addition to, windowing applied in a receiver. The output of the circuit **204** may comprise C samples of the received signal corresponding to a particular OFDM symbol received across C+Δ subcarriers.

The frequency correction circuit **206** may be operable to adjust a frequency of signal **205** to compensate for frequency errors which may result from, for example, limited accuracy of frequency sources used for up and down conversions. The frequency correction may be based on feedback signal **223** from the carrier recovery circuit **222**.

The serial-to-parallel conversion circuit **208** may be operable to convert C time-domain samples output serially as the signal **207** to C time-domain samples output in parallel as signals **209**.

In an example implementation, where interleaving of the subcarrier values was performed in transmitter, the phase/

frequency-corrected, equalized subcarrier values output at link **215** may be de-interleaved prior to being input to the circuit **218** and/or the circuit **216** may perform de-interleaving of the subcarrier values. In this case the Controlled ISCI Model **220** (comprising the combined ISC model used by the modulator and/or ICI model reflecting the channel non-idealities) should consider the interleaving operation.

Each of the signals **203**, **205**, **207**, and **209** may be time-domain signals. The fast Fourier transform (FFT) circuit **210** may be operable to convert the time-domain samples conveyed as signals **209** to C physical subcarrier values conveyed as signals **211**.

The per-tone equalizer **212** may be operable to perform frequency-domain equalization of each of the C physical subcarrier values to compensate for non-idealities (e.g., multipath, additive white Gaussian noise, (AWGN), etc.) experienced by a corresponding one of the C OFDM subcarriers. In an example implementation, the equalization may comprise multiplying a sample of each of signals **211** by a respective one of C complex coefficients determined by the equalization circuit **212**. Such coefficients may be adapted from OFDM symbol to OFDM symbol. Adaption of such coefficients may be based on decisions of decoding circuit **218**. In an example implementation, the adaptation may be based on an error signal **221** defined as the difference, output by circuit **230**, between the equalized and phase-corrected samples of signal **217** and the corresponding reconstructed signal **227***b* output by the decoding circuit **218**. Generation of the reconstructed signal **227***b* may be similar to generation of the reconstructed signal **203** in the above-incorporated U.S. patent application Ser. No. 13/754,964 (but modified for the OFDM case, as opposed to the single-carrier case described therein) and/or as described below with reference to FIG. **2**D.

The phase correction circuit **214** may be operable to adjust the phase of the received physical subcarrier values. The correction may be based on the feedback signal **225** from the carrier recovery circuit **222** and may compensate for phase errors introduced, for example, by frequency sources in the front-end of the transmitter and/or the front-end **202** of the receiver.

The parallel-to-serial conversion circuit **216** may convert the C physical subcarrier values output in parallel by circuit **214** to a serial representation. The physical subcarrier values bits may then be conveyed serially to the decoding circuit **218**. Alternatively, **216** may be bypassed (or not present) and the decoding at **218** may be done iteratively over the parallel (vector) signal **215**.

The controlled ISCI model circuit **220** may be operable to store tap coefficients $\underline{p}$ and/or nonlinearity model $\widehat{NL}$ The stored values may, for example, have been sent to the receiver **200** by the transmitter **100** in one or more control messages. The controlled ISCI model circuit **220** may be operable to convert a time-domain representation of a nonlinearity model to a frequency domain representation. The model **220** may, for example, store (e.g., into a look-up table) multiple sets of filter coefficients and/or nonlinearity models and may be operable to dynamically select (e.g., during operation based on recent measurements) the most appropriate one(s) for the particular circumstances.

The decoding circuit **218** may be operable to process the signal **217** to recover symbols carried therein. In an example implementation, the decoding circuit **218** may be an iterative maximum likelihood or maximum a priori decoder that uses symbol slicing or other techniques that enable estimating individual symbols rather than sequences of symbols. In another example implementation, the decoding circuit **218** may be a sequence estimation circuit operable to perform sequence estimation to determine the C' symbols that were generated in the transmitter corresponding to the received OFDM symbol. Such sequence estimation may be based on maximum likelihood (ML) and/or maximum a priori (MAP) sequence estimation algorithm(s), including reduced-complexity (e.g., storing reduced channel state information) versions thereof. The decoding circuit **218** may be able to recover the C' symbols from the C physical subcarriers (where C'>C) as a result of the controlled inter-symbol correlation and/or aliasing that was introduced by the transmitter (e.g., as a result of the processing by the ISC generation circuit **104** and/or the aliasing introduced by the decimation circuit **108**). The decoding circuit **218** may receive, from circuit **220**, a frequency-domain controlled ISCI model which may be based on non-linearity, phase noise, and/or other non-idealities experienced by one or more of the C physical subcarrier values arriving at the decoding circuit **218**.

The decoding circuit **218** may use the controlled ISCI model to calculate metrics similar to the manner in which a model is used to calculate metrics in above-incorporated U.S. patent application Ser. No. 13/754,964 (but modified for the OFDM case as opposed to the single-carrier case described therein) and/or as described below with reference to FIG. **2**C. The decoding circuit **218** may also use the controlled ISCI model provided by circuit **220** to generate signals **227***a* and **227***b*, as described herein. In an example implementation, the decoding circuit **218** is operable to get at its input C equalized and phase-corrected physical subcarrier values and generate LLR values associated with the bits of the C' constellation symbols that where originally loaded over the virtual subcarriers of the WAM-OFDM transmitter. The LLRs may be generated by checking multiple hypotheses of C' constellation symbols based on the received samples. The best hypothesis may be used to generate the symbols and hard bits detection. In case of using a soft error correction code, an LLR interface that reflects the reliability of the bits (analog signal) rather than the hard bits (i.e., "0", "1") may be used. A remaining one or more of the hypotheses (the second-best, third-best, etc.) may be used to generate the LLR values. For example, assuming that a particular bit was detected as "1" according to the best hypothesis, the LLR for this bit may be provided from the distance of the best hypothesis to the second best hypothesis that estimates this particular bit as "0". The LLR values for the different virtual subcarriers may be weighted according to their respective SNR. In case of frequency-selective fading channel, each subcarrier may have a different gain that corresponds to a different SNR per subcarrier. Because LLR value reflects the bit reliability, in an example implementation, the LLRs may be weighted according to the appropriate subcarrier gain to achieve Maximum Likelihood performance. In an example implementation, log-likelihood ratios (LLRs) determined in a receiver (e.g., in circuit **218**) may have a noise variance component that varies with subcarrier. This may be because the per-subcarrier channel gain (due, for example, to the analog channel selection filter circuits and channel) may vary with frequency but the RF front-end gain at the receiver may be fixed.

For each received OFDM symbol, the circuit **220** may generate a frequency-domain controlled ISCI model of the channel over which the OFDM symbol was received. The controlled ISCI model of **220** may account for non-linear distortion experienced by the received OFDM symbol, phase noise experienced by the received OFDM symbol, and/or other non-idealities. For example, a third-order time domain distortion may be modeled in the frequency domain as:

$$y(t) = x(t) \cdot (1 - r \cdot e^{j\varphi} \cdot |x(t)|^2) = x(t) - r \cdot e^{j\varphi} \cdot x(t) \cdot x^*(t) \cdot x(t)$$

$$Y(\omega) = X(\omega) - r \cdot e^{j\varphi} \cdot X(\omega) \otimes X^*(-\omega) \otimes X(\omega),$$

where:

x(t), X(ω)—are the input signal in the time domain and frequency domain, respectively;

y(t), Y(ω)—are the distorted output signal in the time domain and frequency domain, respectively;

$r \cdot e^{j\Phi}$—is the complex distortion coefficients;

( )*—denotes complex conjugate operator; and

⊗—stands for the convolution operator.

The carrier recovery loop circuit **222** may be operable to recover phase and frequency of one or more of the C OFDM subcarriers of the channel **120**. The carrier recovery loop **222** may generate a frequency error signal **223** and a phase error signal **225**. The phase and/or frequency error may be determined by comparing physical subcarrier values of signal **217** to a reconstructed signal **227***a*. Accordingly, the frequency error and/or phase error may be updated from OFDM symbol to OFDM symbol. The reconstructed signal **227***b* may be generated similar to the manner in which the reconstructed signal **207** of the above-incorporated U.S. patent application Ser. No. 13/754,964 (but modified for the OFDM case, as opposed to the single-carrier case described therein) and/or as described below with reference to FIG. **2**D.

The performance indicator measurement circuit **234** may be operable to measure, estimate, and/or otherwise determine characteristics of received signals and convey such performance measurement indications to a transmitter collocated with the receiver **200** for transmitting the feedback to the remote side. Example performance indicators that the circuit **234** may determine and/or convey to a collocated transmitter for transmission of a feedback signal include: signal-to-noise ratio (SNR) per subcarrier (e.g., determined based on frequency-domain values at the output of FFT **210** and corresponding decisions at the output of the decoding circuit **218** and/or FEC decoder **232**), symbol error rate (SER) (e.g., measured by decoding circuit **218** and conveyed to the circuit **234**), and/or bit error rate (BER) (e.g., measured by the FEC decoder and conveyed to the circuit **234**).

FIGS. **2**B and **2**C depict a flowchart describing operation of an example implementation of a highly-spectrally-efficient OFDM receiver. The process begins with block **242** in which an OFDM symbol arrives, as signal **121**, at front-end **202** and is amplified, down-converted, and digitized to generate C+Δ+P time-domain samples of the OFDM symbol, where P is the size of the cyclic prefix.

In block **244**, the cyclic prefix may be removed and a windowing function may be applied.

In block **246**, frequency correction may be applied to the time-domain samples based on an error signal **223** determined by the carrier recovery circuit **222**.

In block **248**, the frequency-corrected time-domain samples are converted to frequency-corrected frequency-domain physical subcarrier values by the FFT circuit **210**.

In block **250**, the frequency-corrected physical subcarrier values output by the FFT are equalized in the frequency domain by the per-subcarrier equalizer circuit **212**.

In block **252**, one or more of the frequency-corrected and equalized physical subcarrier values are phase corrected based on a phase correction signal **225** generated by the carrier recovery circuit **222**.

In block **254**, the vector of C frequency-corrected, equalized, and phase-corrected received physical subcarrier values is input to decoding circuit **218** and sequence estimation is used to determine the best estimates of the vector of C' symbols that resulted in the vector of C frequency-corrected, equalized, and phase-corrected received physical subcarrier values. Example details of metric generation performed during the sequence estimation are described below with reference to FIG. **2**C.

In block **256**, the best estimate of the vector of C' symbols is determined by decoding circuit **218** and is output as signal **219** to FEC decoder **232**, which outputs corrected values on signal **233**. Example details of selecting the best candidate vector are described below with reference to FIG. **2**C.

Referring to FIG. **2**C, in block **262**, the decoding circuit **218** generates a plurality of candidate vectors (each candidate vector corresponding to a possible value of the vector of C' symbols generated by the transmitter), and generates a corresponding plurality of reconstructed physical subcarrier vectors by applying the controlled ISCI model to the candidates.

In block **264**, the reconstructed physical subcarrier vectors are compared to the vector of frequency-corrected, equalized, and/or phase-corrected received physical subcarrier values to calculate metrics.

In block **266**, the candidate vector corresponding to the best metric is selected as the best candidate, and the C' symbols of the best candidate are output as signal **219**, to, for example, FEC decoder **232** and/or an interleaver (not shown).

FIG. **2**D depicts a flowchart describing operation of an example decoding circuit of a highly-spectrally-efficient OFDM receiver. The flowchart begins with block **272** in which a vector of C received physical subcarrier values arrive at decoding circuit **218**.

In block **274**, the best candidate vector is determined to a first level of confidence. For example, in block **274**, the best candidate vector may be determined based on a first number of iterations of a sequence estimation algorithm.

In block **276**, the controlled ISCI model may be applied to the best candidate vector determined in block **274** to generate reconstructed signal **227***a*.

In block **278**, the best candidate vector is determined to a second level of confidence. For example, the best candidate determined in block **278** may be based on a second number of iterations of the sequence estimation algorithm, where the second number of iterations is larger than the first number of iterations.

In block **280**, the controlled ISCI model may be applied to the best candidate determined in block **278** to generate reconstructed signal **227***b*.

In block **282**, coefficients used by the equalizer **212** are updated/adapted based on the reconstructed signal **227***b* determined in block **280**.

In block **284**, subsequent received physical subcarrier values are equalized based on the coefficients calculated in block **282**.

Blocks **286** and **288** may occur in parallel with blocks **278**-**284**.

In block **286**, the carrier recovery loop **222** may determine frequency and/or phase error based on signal **227***a* calculated in block **276**.

In block **288**, samples received during a subsequent OFDM symbol period may be frequency corrected based on the error determined in block **286** and/or subsequent received physical subcarrier values are phase corrected based on the error determined in block **286**.

In an example implementation, a first electronic device (e.g., 100), may map, using a selected modulation constellation, each of C' bit sequences to a respective one of C' symbols, where C' is a number greater than one. The electronic

device may process the C' symbols to generate C' inter-carrier correlated virtual subcarrier values. The electronic device may decimate the C' virtual subcarrier values down to C physical subcarrier values, C being a number less than C'. The electronic device may transmit the C physical subcarrier values on C orthogonal frequency division multiplexed (OFDM) subcarriers. The transmission may be via a channel having a significant amount of nonlinearity. The significant amount of nonlinearity may be such that it degrades, relative to a perfectly linear channel, a performance metric in said receiver by less than 1 dB, whereas, in a full response communication system, it would degrade, relative to a perfectly linear channel, the performance metric by 1 dB or more. The processing may introduce a significant amount of aliasing such that the ratio of the signal power of the C' virtual subcarrier values prior to the decimating to the signal power of the C physical subcarrier values after the decimating is equal to or less than a threshold signal to noise ratio of a receiver to which the OFDM subcarriers are transmitted (e.g., for a decimation by a factor of 2, P2 is the power in the upper half of the C' virtual subcarrier values). The modulation constellation may be an N-QAM constellation, N being an integer. The bit sequences may be coded according to a forward error correction algorithm. The processing may comprise multiplication of C' symbols by a C'×C' matrix. Row or column length of the matrix may be an integer less than C', such that the multiplication results in a decimation of the C' symbols. The processing may seeks to achieve a target symbol error rate, target bit error rate, and/or target packet error rate in presence of additive white Gaussian noise and a dynamic frequency selective fading channel. The processing may comprises filtering the C' symbols using an array of filter tap coefficients. The filtering may comprise cyclic convolution. The filtering may comprises multiplication by a circulant matrix populated with the filter tap coefficients. The filter tap coefficients may be selected to achieve one or more of: a target symbol error rate, a target bit error rate, and/or a target packet error rate in presence of one or more of: additive white Gaussian noise, dynamic frequency selective fading channel, and non-linear distortion. The filter tap coefficients may be selected based on signal-to-noise ratio (SNR) measurements fed back from a second electronic device that receives communications from the first electronic device.

The electronic device may receive a first message from a second electronic device. In response to the first message, the first electronic device may cease transmission of data on a particular one of the physical subcarriers. The electronic device may receive a second message from the second electronic device. In response to the second message, the first electronic device may resume transmission of data on the particular one of the physical subcarriers. Subsequent to the receiving the first message, and prior to receiving the second message, transmitting a pilot signal on the particular one of the physical subcarriers. The ceasing transmission of data on the particular one of the physical subcarriers may comprise one or more of: changing a value of the number C; and changing a value of the number C'. An OFDM symbol period for the transmitting may be approximately (C+Δ)/BW. Each of the C OFDM subcarriers has a bandwidth of approximately BW/(C+Δ), where BW is a bandwidth used for the transmitting, and Δ is the number of non-data-carrying subcarriers within the bandwidth BW. Prior to the transmitting, transforming the C physical subcarrier values to C+Δ+P time-domain samples using an inverse fast Fourier transform.

Other implementations may provide a non-transitory computer readable medium and/or storage medium, and/or a non-transitory machine readable medium and/or storage medium, having stored thereon, a machine code and/or a computer program having at least one code section executable by a machine and/or a computer, thereby causing the machine and/or computer to perform the processes as described herein.

Methods and systems disclosed herein may be realized in hardware, software, or a combination of hardware and software. Methods and systems disclosed herein may be realized in a centralized fashion in at least one computing system, or in a distributed fashion where different elements are spread across several interconnected computing systems. Any kind of computing system or other apparatus adapted for carrying out the methods described herein is suited. A typical combination of hardware and software may be a general-purpose computing system with a program or other code that, when being loaded and executed, controls the computing system such that it carries out methods described herein. Another typical implementation may comprise an application specific integrated circuit (ASIC) or chip with a program or other code that, when being loaded and executed, controls the ASIC such that is carries out methods described herein.

While methods and systems have been described herein with reference to certain implementations, it will be understood by those skilled in the art that various changes may be made and equivalents may be substituted without departing from the scope of the present method and/or system. In addition, many modifications may be made to adapt a particular situation or material to the teachings of the present disclosure without departing from its scope. Therefore, it is intended that the present method and/or system not be limited to the particular implementations disclosed, but that the present method and/or system will include all implementations falling within the scope of the appended claims.

What is claimed is:

1. A system comprising:

a symbol mapper circuit that outputs C' quadrature amplitude modulation (QAM) symbols per orthogonal frequency division multiplexing (OFDM) symbol;

circuitry operable to process said C' QAM symbols using a circulant matrix to generate a particular OFDM symbol consisting of C+Δ subcarriers, where C' is a first integer, C is a second integer less than C', and Δ is an integer equal to the number of non-data-carrying subcarriers in said particular OFDM symbol, wherein:

said circuitry comprises a filter;

elements of said circulant matrix are equal to coefficients of said filter;

said filter is operable to filter said C' QAM symbols to introduce inter-symbol correlation among said C' QAM symbols.

2. The system of claim **1**, wherein said circulant matrix is a P×P matrix, where P is an integer less than C'.

3. The system of claim **1** comprising a nonlinear circuit that introduces nonlinear distortion to said particular OFDM symbol, wherein said nonlinear distortion impacts a performance metric by 1 dB or more.

4. The system of claim **1**, wherein one or more parameters that determine an amount of nonlinear distortion introduced by said nonlinear circuit are configurable.

5. The system of claim **4**, wherein said circuitry is operable to configure one or more values of said one or more parameters during operation of said nonlinear circuit.

6. The system of claim **5**, wherein said circuitry is operable to transmit said one or more values of said one or more parameters such that said one or more values are available for use by a receiver of said OFDM symbol in modeling said nonlinear distortion.

7. The system of claim 1 wherein said circuitry is operable to cease transmission of data on a one or more of said C+Δ subcarriers in response to a first feedback message from a receiver.

8. The system of claim 7, wherein said circuitry is operable resume transmission of data on said one or more of said C+Δ subcarriers in response to a second feedback message from a receiver.

9. A method comprising:

in an electronic receiver:

outputting, by a symbol mapper circuit, C' quadrature amplitude modulation (QAM) symbols per orthogonal frequency division multiplexing (OFDM) symbol;

processing, via circuitry of said receiver, said C' QAM symbols using a circulant matrix to generate a particular OFDM symbol consisting of C+Δ subcarriers, where C' is a first integer, C is a second integer less than C', and Δ is an integer equal to the number of non-data-carrying subcarriers in said particular OFDM symbol, wherein:

said circuitry comprises a filter; and

elements of said circulant matrix are equal to coefficients of said filter; and

filtering, by said filter, said C' QAM symbols to introduce inter-symbol correlation among said C' QAM symbols.

10. The method of claim 9, wherein said circulant matrix is a P×P matrix, where P is an integer less than C'.

11. The method of claim 9 comprising, in a nonlinear circuit of said electronic receiver, introducing nonlinear distortion to said particular OFDM symbol, wherein said nonlinear distortion impacts a performance metric by 1 dB or more.

12. The method of claim 9, wherein one or more parameters that determine an amount of nonlinear distortion introduced by said nonlinear circuit are configurable.

13. The method of claim 12, comprising configuring, by said circuitry, one or more values of said one or more parameters during operation of said nonlinear circuit.

14. The method of claim 13, comprising transmitting, by said circuitry, said one or more values of said one or more parameters such that said one or more values are available for use by a receiver of said OFDM symbol in modeling said nonlinear distortion.

15. The method of claim 9 comprising, performing by said circuitry, ceasing transmission of data on a one or more of said C+Δ subcarriers in response to a first feedback message from a receiver.

16. The method of claim 15, comprising, performing by said circuitry, resuming transmission of data on said one or more of said C+Δ subcarriers in response to a second feedback message from a receiver.

* * * * *